Proc. Natl. Acad. Sci. USA
Vol. 96, pp. 2621–2626, March 1999
Applied Biological Sciences

Structural characteristics of supramolecular assemblies formed by guanidinium-cholesterol reagents for gene transfection

BRUNO PITARD*†, NOUFISSA OUDRHIRI‡, JEAN-PIERRE VIGNERON§, MICHELLE HAUCHECORNE‡, OLIVIER AGUERRE¶, RENÉE TOURY‡, MARC AIRIAU¶, RAJEN RAMASAWMY‡, DANIEL SCHERMAN*, JOËL CROUZET‖, JEAN-MARIE LEHN§, AND PIERRE LEHN‡

*Unité Mixte de Recherche, 133 Rhône-Poulenc Rorer, Centre National de la Recherche Scientifique, ‖Rhône-Poulenc Rorer Gencell, 13 quai Jules Guesde, BP 14, 94403 Vitry-sur-Seine Cedex, France; ‡Institut National de la Santé et de la Recherche Médicale, Unité 458, Hôpital Robert Debré, 48 Boulevard Sérurier, 75019 Paris, France; §Laboratoire de Chimie des Interactions Moléculaires, Collège de France, 11 Place Marcelin Berthelot, 75005 Paris, France; ¶Rhodia, 52 rue de la Haie Coq, 93309 Aubervilliers, France

Contributed by Pierre Lehn, December 10, 1998

ABSTRACT **We have recently discovered that cationic cholesterol derivatives characterized by guanidinium polar headgroups are very efficient for gene transfection *in vitro* and *in vivo*. In spite of being based on some rationale at the molecular level, the development of these new synthetic vectors was nevertheless empirical. Indeed, the factors and processes underlying cationic lipid-mediated gene transfer are still poorly understood. Thus, to get a better insight into the mechanisms involved, we have examined the supramolecular structure of lipid/DNA aggregates obtained when using reagent bis(guanidinium)-tren-cholesterol (BGTC), either alone or as a liposomal formulation with the neutral phospholipid dioleoyl phosphatidylethanolamine (DOPE). We here report the results of cryotransmission electron microscopy studies and small-angle x-ray scattering experiments, indicating the presence of multilamellar domains with a regular spacing of 70 Å and 68 Å in BGTC/DOPE–DNA and BGTC–DNA aggregates, respectively. In addition, DNA lipoplexes with similar lamellar patterns were detected inside transfected HeLa cells by conventional transmission electron microscopy. These results suggest that DNA condensation by multivalent guanidinium-cholesterol cationic lipids involves the formation of highly ordered multilamellar domains, the DNA molecules being intercalated between the lipid bilayers. These results also invite further investigation of the intracellular fate of the internalized lipid/DNA structures during their trafficking toward the cell nucleus. The identification of the basic features of active complexes should indeed help in the design of improved guanidinium-based vectors.**

Over the last several years, various gene delivery systems have been investigated for gene therapy approaches of both inherited and acquired diseases. Most work has focused on the use of recombinant viruses. Viruses can indeed be viewed as precise nucleic acid-containing macromolecular assemblies characterized by sophisticated structural features that have been adjusted by natural evolution to allow efficient infection by means of appropriate interactions with the molecular machinery of their host cells (1). However, viral vectors also have a number of disadvantages, including safety concerns and practical issues relating to bulk production and quality control. As a consequence, various methods for nonviral gene delivery have also been considered and very actively investigated.

Among the synthetic vectors, cationic lipids are particularly attractive, because it is possible to design and synthesize a great variety of reagents with favorable features such as simplicity of use, biodegradability, relatively high transfection activity, etc. (2). Many different cationic lipids are at present commercially available and several lipid formulations have already been used in the clinical setting. However, there is still limited understanding of the factors and processes leading to transfection that determine its efficiency. Thus, cationic lipids are generally developed on the basis of trial and error by using expression of the transgene as the end point.

We have recently discovered that cationic cholesterol derivatives bearing guanidinium polar headgroups are efficient and versatile reagents for gene transfer. Reagent bis(guanidinium)-tren-cholesterol [tren, tris(2-aminoethyl)amine] (BGTC) was shown to be efficient in promoting gene transfer into numerous mammalian cell lines and also into primary human airway cells *in vitro*; BGTC/dioleoyl phosphatidyl ethanolamine (DOPE) liposomes were found to mediate gene transfection into the mouse airway epithelium *in vivo* (3, 4).The rationale (at the molecular level) underlying our approach was that such cationic cholesterol derivatives should combine the membrane-compatible features of the cholesterol moiety and the highly favorable features of the guanidinium function for DNA binding (3, 5).

Most importantly, because gene transfection by cationic lipids involves the spontaneous *in vitro* formation of discrete lipid/DNA particles, the transfection efficacy of a given cationic lipid system also highly depends on the structural and functional properties of the self-assembled supramolecular assemblies. In fact, the features of the formed lipoplexes are directly related to the physicochemical properties of the component lipids. Accordingly, characterization of the structure of the lipoplexes should help toward a better understanding of the mechanisms of BGTC-mediated lipofection.

Therefore, we examined the supramolecular structure of DNA aggregates obtained by mixing plasmid DNA with reagent BGTC used either alone or as a liposomal formulation with the neutral helper lipid DOPE. We here report data from cryotransmission electron microscopy (cryo-TEM) studies and small-angle x-ray scattering (SAXS) experiments showing the presence of multilamellar domains in both types of DNA aggregates. In addition, by using conventional TEM, we observed lipoplexes exhibiting a similar lamellar pattern inside transfected HeLa cells.

MATERIALS AND METHODS

Cationic Lipids, Plasmids, and Preparation of Lipoplexes. The cationic lipid BGTC was synthesized as previously de-

The publication costs of this article were defrayed in part by page charge payment. This article must therefore be hereby marked "*advertisement*" in accordance with 18 U.S.C. §1734 solely to indicate this fact.

PNAS is available online at www.pnas.org.

Abbreviations: BGTC, bis(guanidinium)-tren-cholesterol [tren, tris(2-aminoethyl)amine]; DOPE, dioleoyl phosphatidyl ethanolamine; SAXS, small-angle x-ray scattering; TEM, transmission electron microscopy; DOTAP, dioleoyl trimethylammonium propane; DOPC, dioleoyl phosphatidylcholine.

†To whom reprint requests should be addressed. e-mail: bruno.pitard@rp-rorer.fr.

scribed (3). BGTC dispersions were obtained by heating a 10-mM aqueous solution of BGTC for 30 min at 50°C. BGTC/DOPE liposomes (molar ratio 3/2) were prepared as described in ref. 3 with minor changes, i.e., the dispersion was extruded through 0.2 μm inorganic membrane Whatman Anotop filters.

Plasmid pCMV-Luc (4,500 bp), where the firefly *Photinus pyralis* luciferase gene is driven by the immediate early promoter of the cytomegalovirus, was amplified in *Escherichia coli* and prepared by double-cesium chloride gradient purification by using standard techniques (6).

BGTC/DOPE–DNA aggregates and BGTC–DNA lipoplexes were prepared by mixing equal volumes of BGTC/DOPE liposomes and BGTC solutions respectively at different concentrations, with the plasmid DNA solution at the desired concentration.

Dynamic Light Scattering. Dynamic light scattering analyses were performed by using a Coulter N4-Plus apparatus. Samples were prepared at 10 μg DNA per ml in 150 mM NaCl.

Fluorescence Studies. Fluorescence measurements were carried out on a Jobin-Yvon Spex fluoromax-2 spectrofluorometer (Longjumeau, France). Fluorescence was monitored immediately after addition of ethidium bromide (at a final concentration of 5 μM) to solutions containing 10 μg DNA per ml in 150 mM NaCl. Sample readings were conducted at an excitation wavelength of 260 nm and an emission wavelength of 590 nm. Values were expressed as arbitrary fluorescence units.

Cryo-TEM. Cryo-TEM experiments were performed as described previously (7). Samples were prepared at 0.25 mg DNA per ml in 20 mM NaCl and subsequently concentrated by ultrafiltration by using 300 K nanosep concentrators (Pall). Samples were examined with a Philips (Eindhoven, the Netherlands) CM12 transmission electron microscope.

SAXS. Samples were prepared as described in ref. 7. Briefly, cationic lipid/DNA lipoplexes were prepared at a ratio of 10 nmols BGTC/μg DNA at 0.25 mg DNA per ml in low ionic strength, i.e., 20 mM NaCl, to have highly concentrated soluble colloids (see below). Lipoplexes were concentrated by ultracentrifugation at 400,000 $\times$ *g* for 30 min. Pellets were introduced into a cell comprising two Kapton windows. SAXS experiments were carried out by using the synchrotron radiation source of Laboratoire pour l'Utilisation du Rayonnement Electromagnétique (LURE, Orsay, France) on beamline D43. A two-dimensional image plate detector was used. Results are expressed in arbitrary intensity units of scattering intensity as a function of q, where q is the momentum transfer $q = (4\pi/\lambda)\sin\theta/2$; θ, the scattering angle and λ, the x-ray wavelength. q values ranged between 0.05 $Å^{-1}$ and 0.40 $Å^{-1}$.

Gold-Labeled DNA. Plasmid DNA was biotinylated by using either photoactivatable biotin (Pierce) or the Fast-Tag labeling system (Vector Laboratories). Biotinylated DNA was precipitated and, after centrifugation, the nucleic acid pellet was resuspended in water. Finally, a solution of 30 μg of the biotinylated plasmid was incubated for 30 min with 1 ml of AuroProbe EM Streptavidin G15 (Amersham).

Cell Culture and Transfection Procedure. HeLa cells were cultured and transfected as previously described (3). Particularly, 5 μg of gold-labeled plasmid pRSV-Luc was mixed with an amount of reagent BGTC or BGTC/DOPE liposomes known to be optimal for *in vitro* gene transfection (3).

Conventional Electron Microscopy. Conventional TEM studies were performed on HeLa cells transfected with either unlabeled or gold-labeled plasmid DNA complexed with BGTC alone or BGTC/DOPE liposomes. Briefly, HeLa cells were fixed *in situ* at various times (ranging from 1 to 24 hr) after transfection with 1% glutaraldehyde for 1 hr at 4°C and processed by using standard EM procedures. The samples were postfixed in 2% osmium tetroxide for 1 hr and then dehydrated in a graded series of ethanol washes. Cells were embedded in Epon 812 (Electron Microscopy Sciences, Fort Washington, PA). Ultrathin (80 nm) sections were stained with 5% uranyl acetate and Reynold's lead citrate. Finally, sections were examined by using a Philips EM201 transmission electron microscope.

RESULTS

Colloidal Stability, Cryo-TEM, and SAXS of BGTC/DOPE–DNA Lipoplexes. Because stability of the lipoplexes is a major requirement for gene transfection, we first studied the colloidal stability of BGTC/DOPE–DNA aggregates. A parameter playing a key role in colloidal stability is the charge ratio of the lipoplexes, i.e., the ratio of positive charge equivalents to negative charge equivalents. When taking into account that 1 μg of DNA is 3 nmols of negatively charged phosphate and assuming that only the two guanidinium groups (and not the tertiary amine) of BGTC are positively charged at neutral pH, the charge ratio corresponds to 2/3 of the nmols BGTC/μg DNA ratio. Thus, we evaluated the colloidal stability of BGTC/DOPE–DNA lipoplexes using dynamic light scattering. The mean diameter of unreacted BGTC/DOPE liposomes was 150 nm, a value consistent with the diameter determined by cryo-TEM (Fig. 1*A*). BGTC/DOPE–DNA lipoplexes, prepared at different BGTC/DNA ratios and at a DNA concentration similar to that used for *in vitro* transfection, were found to exhibit a three-zone model of colloidal stability (Fig. 2*A*). Of note, we previously reported a similar observation for lipopolyamine/DNA lipoplexes (7). The three different zones, termed A, B, and C, were determined by the concentration of reagent BGTC. In zone A, i.e., for a nmols BGTC/μg DNA ratio below 2, we found colloidally stable lipoplexes with a mean diameter of about 200 nm. In zone B, characterized by BGTC/DNA ratios ranging from 2 to 5 nmols BGTC/μg DNA, the formed lipoplexes were not colloidally stable, as evidenced by the observation that their diameter increased to more than 700 nm in less than 1 hr. Finally, in zone

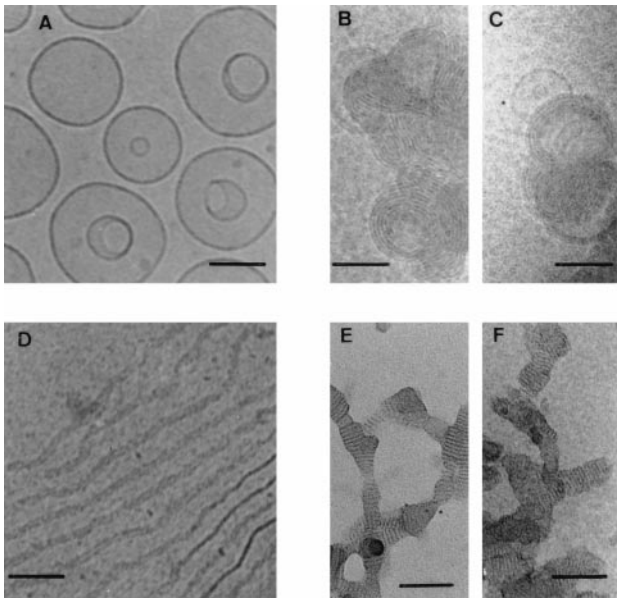

FIG. 1. Cryo-TEM micrographs of BGTC/DOPE liposomes, BGTC/DOPE–DNA lipoplexes, BGTC and BGTC–DNA lipoplexes. (*A*) Unreacted BGTC/DOPE liposomes at 10 mM BGTC in 20 mM Hepes, pH 7.4. (*B* and *C*) BGTC/DOPE–DNA lipoplexes from zone C (10 nmols BGTC/μg DNA). (*D*) Lipid BGTC in aqueous solution. (*E* and *F*) Cryophosphotungstate-TEM micrographs of BGTC–DNA lipoplexes from zone C (10 nmols BGTC/μg DNA). The sample was mixed with phosphotungstate just before water vitrification to enhance the contrast. Scale bar: 100 nm.

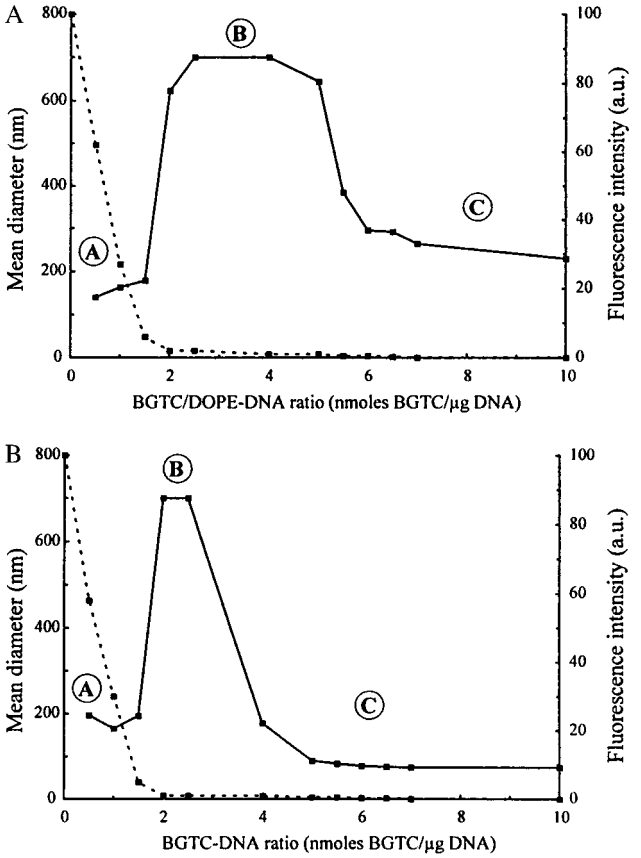

FIG. 2. Dynamic light-scattering analysis (solid line) to assess colloidal stability of the lipoplexes. Size determination was performed after 1 hr of complexation at room temperature; lipoplexes from zones A and C were stable, whereas those from zone B exhibited a visible precipitate. Fluorescence measurements (dashed line) to assess DNA entrapment in the lipoplexes. BGTC/DOPE–DNA lipoplexes (*A*) and BGTC-DNA lipoplexes (*B*) at BGTC/DNA ratios ranging from 0 to 10.

C, i.e., for a nmols BGTC/μg DNA ratio above 5 (highly positive complexes), we observed colloidally stable lipoplexes, the diameter of which decreased (from 650 to 250 nm) with increasing concentrations of BGTC (Fig. 2*A*). Interestingly, we have previously reported that such highly positive lipoplexes were optimal for *in vitro* gene transfection and could also be used for gene transfer into mouse airways (3, 4).

Fluorescence experiments were performed to evaluate DNA entrapment in the formed aggregates. Thus, BGTC/DOPE–DNA lipoplexes were exposed to ethidium bromide, which on intercalation between DNA base pairs acts as a fluorescence probe. Fig. 2*A* shows fluorescence intensity as a function of the BGTC/DNA ratio. Fluorescence intensity sharply decreased in zone A from 100% to a value close to zero and stayed at this minimum level in zones B and C. This indicates that part of the plasmid DNA was accessible to the probe in zone A; on the contrary, in zones B and C, the fluorescence level was minimal because of total entrapment of all DNA molecules in the lipoplexes. Accordingly, when probing the BGTC/DOPE–DNA lipoplexes by agarose gel electrophoresis, no ethidium bromide staining of DNA was observed with complexes characterized by a charge ratio above 1.6. In addition, we also observed that lipoplexes from zones B and C were fully protected from degradation by DNase I (data not shown).

To visualize the structural features of the lipoplexes formed at lipid/DNA ratios that are typically used for transfection, we used cryo-TEM, because it allows imaging of bioassemblies close to their native state. Thus, we performed cryo-TEM studies on unreacted BGTC/DOPE liposomes and on lipoplexes from zone C. Cryo-TEM examination of unreacted BGTC/DOPE liposomes showed a fairly homogeneous population of unilamellar liposomes about 150 nm in diameter (Fig. 1*A*). Of note, invaginated liposomes were relatively frequent (Fig. 1*A*); as recently suggested by others, this may be related to the occurrence of ionic gradients during sample processing for cryo-TEM experiments and/or to the extrusion step during the liposome preparation (8, 9). Most importantly, cryo-TEM examination of BGTC/DOPE–DNA aggregates from zone C visualized discrete concentric multilamellar structures of approximately 250 nm in diameter (Fig. 1 *B* and *C*).

To characterize further the structural features of BGTC/DOPE–DNA lipoplexes, we also used synchrotron SAXS. In Fig. 3*A*, the scattering intensity of BGTC/DOPE–DNA lipoplexes from zone C is plotted as a function of the scattering vector. Importantly, in addition to the strong first-order reflection at 70 Å, a second-order peak at 35 Å could also be easily detected, a finding clearly indicating lamellar organization with a regular spacing of 70 Å. In control experiments, diffraction maxima were exhibited neither by naked plasmid DNA nor by unreacted BGTC/DOPE unilamellar liposomes (data not shown). Thus, the scattering pattern reflects the periodic spacing of lamellar BGTC/DOPE–DNA lipoplexes, the periodicity of 70 Å being consistent with stacks of alternating lipid bilayers and DNA. Measurement of the half-width of the first-order diffraction peak at 70 Å indicated an effective domain size of 260 Å, corresponding to about four periodicities and consistent with cryo-TEM micrographs (Fig. 1 *B* and *C*).

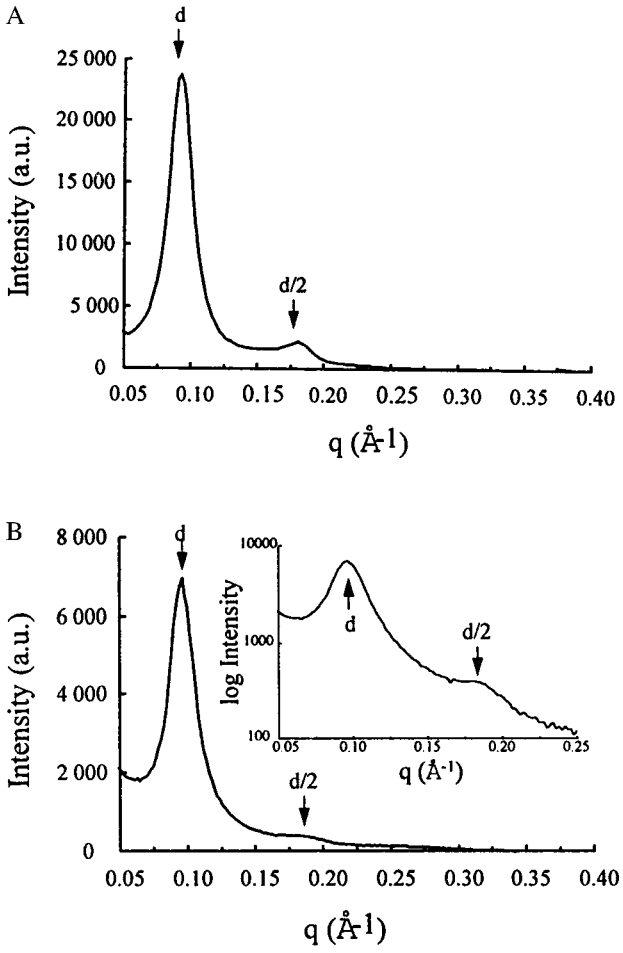

FIG. 3. SAXS scans of BGTC/DOPE–DNA lipoplexes from zone C (*A*) and of BGTC-DNA lipoplexes from zone C (*B*); in the *Inset*, the log of the scattering intensity is plotted as a function of the momentum transfer *q*. d and d/2 correspond to the first reflection and the second order reflection, respectively.

Colloidal Stability, Cryo-TEM, and SAXS of BGTC–DNA Lipoplexes. Similar to BGTC/DOPE–DNA complexes, BGTC–DNA lipoplexes, prepared at different BGTC/DNA ratios, were also found to exhibit a three-zone model of colloidal stability (Fig. 2*B*). The boundary between zone A and zone B was observed at a similar nmols BGTC/μg DNA ratio of 2. However, colloidally stable cationic BGTC/DNA lipoplexes from zone C were obtained for ratios higher than 4 nmols BGTC/μg DNA; thus it is noteworthy that zone B was more extended in the case of BGTC/DOPE–DNA complexes.

As for BGTC/DOPE–DNA lipoplexes, fluorescence experiments showed a sharp decrease in fluorescence intensity when the BGTC/DNA ratio was increased from 0 to 2 nmols BGTC/μg DNA and the fluorescence level remained minimal at higher ratios. This indicates again that part of plasmid DNA was still accessible to ethidium bromide in zone A, whereas in zones B and C all DNA molecules were protected from intercalation of the probe.

Cryo-TEM observation of an aqueous solution of BGTC showed threadlike ribbons about 15 nm in width and 5 nm thick (Fig. 1*D*); these ribbons were very long, i.e., 1 μm, because they were larger than the holes of the perforated carbon film supported by the copper electron microscope grid (data not shown). We also used cryo-TEM to visualize the structures of positive lipoplexes formed at BGTC/DNA ratios (10 nmols/μg DNA) typically used for transfection (3, 4). As shown in Fig. 1 *E* and *F*, the structural features of BGTC/DNA lipoplexes were obviously quite different from the concentric multilamellar vesicles of cationic BGTC/DOPE–DNA complexes. Indeed, it appears that BGTC–DNA lipoplexes rather form ordered domains characterized by a fingerprint-like repetition of flat lines (without obvious circles), a finding suggesting lamellar organization. Of note, these fingerprint-like ordered domains appeared to be connected.

SAXS scans of positive BGTC–DNA lipoplexes showed a strong diffraction band at 68 Å and a second-order peak at 34 Å, corresponding to a lamellar organization with a regular spacing of 68 Å (Fig. 3*B*). As controls, unreacted BGTC and naked DNA did not give any x-ray diffraction peak (data not shown).

TEM of HeLa Cells Transfected with Gold-Labeled DNA Complexed with BGTC–DOPE Liposomes or BGTC Micelles. To assess the relevance of the above structural data for gene transfection, we performed TEM studies of HeLa cells transfected with positively charged DNA aggregates typically used for transfection experiments, the gold-labeled DNA being complexed with either BGTC/DOPE liposomes or BGTC micelles. We used HeLa cells because they are widely used for gene transfection studies and because transgene expression in HeLa cells have been shown to parallel uptake of lipid/DNA complexes (10).

Typical BGTC/DOPE–DNA aggregates were easily detected in intracytoplasmic vesicles. Fig. 4 *A* and *B* show representative examples highlighting the fact that these vesi-

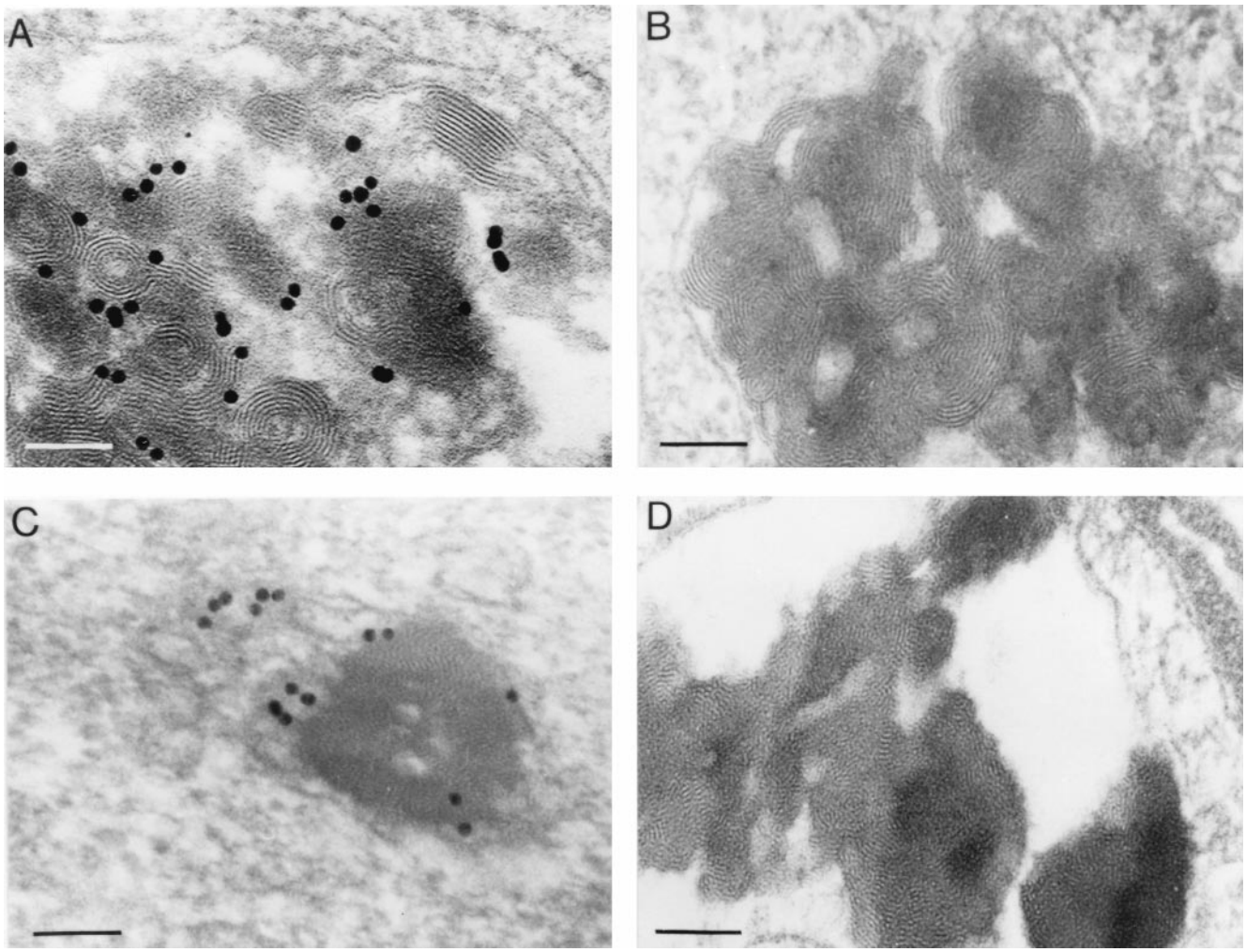

FIG. 4. Electron micrographs of HeLa cells transfected with DNA complexed with BGTC/DOPE liposomes (*A* and *B*) or reagent BGTC (*C* and *D*). In *A* and *C*, plasmid DNA was gold labeled before complexation with the cationic lipid. In *B*, *C,* and *D*, the cells were processed for electron microscopy after 1 hr of exposure to the transfection mixture, whereas they were fixed at 24 hr after transfection in *A*. Scale bar: 100 nm

cles were often quasi-filled by the electron dense lipoplexes. There was a polymorphism with respect to the size of the bioassemblies, because they were composed of variable numbers of individual aggregates. The morphology of the internalized lipoplexes was in general quite similar to that of the lipoplexes imaged by cryo-TEM with a characteristic concentric multilamellar pattern and a negligible inside water space, indicating that the formation of stacked lamellae was the result of the collapse of the liposome structure; of note, optical diffraction on the micrographs showed that the periodicity of the lamellar arrangement was in good agreement with the cryo-TEM and x-ray scattering data (see above and data not shown). These observations strongly suggest that intracellular BGTC/DOPE–DNA lipoplexes also have a lamellar organization with stacks of alternating lipid bilayers and DNA. Observation of typical lipoplexes when using plasmid DNA that had been gold-labeled to allow its identification also suggests that stacks of lipid bilayers are formed to which DNA is adsorbed (Fig. 4*A*). Interestingly, we also noticed that the structural features of the lipoplexes were independent of the conformation and the size of the DNA (data not shown).

BGTC–DNA complexes were also mainly found in intracytoplasmic vesicles in transfected HeLa cells. Their appearance was very similar to that observed by cryo-TEM with ordered multilamellar microdomains. Fig. 4*C* shows a typical aspect of such BGTC–DNA bioassemblies; interestingly, both DNA complexes and individual gold particles seem to be free here in the cytoplasm (possibly after endosomal escape). Identical results were obtained with unlabeled plasmid DNA (Fig. 4*D*).

DISCUSSION

Characterization of the structural features of lipoplexes used for gene transfection is a very active area of research. A hypothetical "bead on string" model in which unmodified cationic liposomes were distinctly attached to the DNA was originally proposed (11). Over the years, various forms of electron microscopy have been used for visualizing different kinds of lipoplexes. Basically, these studies suggested that the DNA was entrapped in condensed structures formed by means of interrelated lipid fusion and DNA collapse (12). These condensed structures were found to exhibit various ordered patterns of supramolecular organization, including multilamellar structures and direct hexagonal tubular packing (13–15). Of note, tubular "spaghetti-like" structures representing a DNA rod coated by a single lipid bilayer were observed in an analysis of the lipoplexes obtained by using the monovalent cationic cholesterol derivative 3-β-[*N*-(*N*′,*N*′-dimethylethane)carbamoyl] cholesterol/DOPE (16, 17).

Most importantly, x-ray diffraction has allowed, in very recent studies, determination of the precise structural characteristics of the lipoplexes resulting from the interaction of DNA with various cationic lipid formulations: lipopolyamine micelles, dioleoyl trimethylammonium propane/dioleoyl phosphatidylcholine (DOTAP/DOPC) liposomes, and dioctadecyldiammonium bromide/cholesterol liposomes (7, 15, 18). It should be stressed here that the structures of the lipoplexes formed by these different cationic lipid formulations were found to consist of a multilamellar membrane in which DNA is intercalated. A periodicity of 8 nm was observed when using a multivalent lipopolyamine reagent formulated as small spherical micelles about 5 nm in diameter, whereas a spacing of 6.5 nm was reported for the lamellar lipoplexes obtained with liposomes containing the monovalent compounds DOTAP and dioctadecyldiammonium bromid (7, 15, 18). Clearly, our data strongly support these previous observations. However, a very recent study showed that DOTAP/DOPE–DNA lipoplexes have an inverted hexagonal organization (19); the formation of a two-dimensional columnar phase was attributed to the presence of DOPE as a multilamellar structure previously found when DOPC was used instead of DOPE (18, 19). It is indeed known that DOPE forms a hexagonal lipid phase, whereas DOPC has a bilayer-forming activity (20, 21). Thus, the fact that BGTC/DOPE–DNA lipoplexes exhibit a lamellar symmetry, whereas DOTAP/DOPE–DNA complexes are packed in an inverted hexagonal phase, may be explained by the important differences existing between DOTAP and BGTC. Indeed, DOTAP bears a single positive quaternary ammonium per molecule, whereas BGTC is a multivalent lipid characterized by a headgroup with guanidinium functions that have characteristic features such as the formation of pairs of parallel hydrogen bonds with phosphate anions and also hydrogen bonding with nucleic bases. In addition, BGTC contains cholesterol, whereas DOTAP has two fatty acids as hydrophobic moiety. It is also interesting to note that the BGTC/DOPE liposomes used in the present study contained a relatively low amount of DOPE because they were characterized by a BGTC/DOPE molar ratio of 3/2; it will thus be important to investigate the structural features (and also the transfection efficiency) of BGTC/DOPE liposomes containing higher amounts of DOPE.

Elucidation of the structural and functional features of the lipoplexes that are the most efficient for gene transfection constitutes a major challenge in the field of cationic lipid-mediated gene delivery. Ideally, this would require determination of not only the initial structural features of the formed lipoplexes but also the precise structural changes that these lipoplexes undergo when they interact with the molecular machinery of the target cells during their trafficking toward the nucleus. It will obviously be difficult to develop such a "supramolecular galenics", especially because of the complexity of the various steps involved. The present study does contribute to the development of this endeavor. First, it is generally agreed that lipoplexes are internalized by means of nonspecific endocytosis after binding of positively charged DNA complexes to anionic residues on the cell surface (10, 14, 22, 23). Thus, detection of typical BGTC/DOPE–DNA and BGTC–DNA structures mainly in intracytoplasmic vesicles of HeLa cells transfected with positively charged aggregates is consistent with electrostatic-driven endocytosis being the major route of DNA uptake during BGTC-mediated transfection. In addition, observation of vesicles quasi-filled with compact lipoplexes could be related to the coalescence of endosomes leading to large membrane-bound vesicles, as already suggested by others (10). Second, as endocytosis leaves the DNA still two membranes away from the nucleus, escape from the endosome and release into the cytosol is a highly critical step that needs to be carried out by the lipoplexes. Previous investigations have suggested that DOPE may play a major role in endosomal escape, because it is a nonbilayer-forming lipid capable of destabilizing the endosomal membrane (21–23). Interestingly, a very recent study has proposed correlation of the high transfection activity of DOTAP/DOPE liposomes and packing of the lipoplexes in an inverted hexagonal phase. It was indeed shown that DOTAP/DOPE–DNA lipoplexes characterized by an inverted hexagonal arrangement fuse and release DNA when in contact with giant anionic vesicles (which are models of cellular membranes), whereas DOTAP/DOPC–DNA complexes (and also DOTAP/DOPE–DNA lipoplexes containing low amounts of DOPE) with a multilamellar structure do so only on a much longer time scale (19). Taken altogether, concentric multilamellar BGTC/DOPE–DNA lipoplexes may escape from intracytoplasmic vesicles by means of membrane disruption, as these complexes might have highly original fusion/destabilization properties, especially because of the multivalent BGTC itself. Thus, it will be important to investigate further such properties of the BGTC/DOPE–DNA lipoplexes, notably by using model membranes. Of note, it has been proposed recently that destabilization of the endosomal membrane may induce the flip-flop of anionic

lipids from the cytoplasm-facing monolayer of the endosome, leading thereby to the formation of a charge-neutral ion pair with the cationic lipid and to subsequent dissociation of the DNA from the complex and its release into the cytoplasm (24). On the other hand, it has been suggested that gene transfection by the lipopolyamine DOGS, a cationic lipid formulation completely devoid of DOPE, involves a different mechanism of endosomal escape: endosome buffering leading to osmotic swelling and endosome disruption (25). Accordingly, as previously suggested, the tertiary amine of BGTC could also buffer the acidic environment of endosomes; endosome buffering may even be a major mechanism of endosomal escape in BGTC-mediated transfection, as BGTC–DNA lipoplexes do not contain DOPE.

Finally, it is tempting to suggest that multilamellar lipoplexes may play an important role in gene transfection by BGTC/DOPE (molar ratio 3/2) liposomes and BGTC micelles. However, it should be stressed that, to verify this hypothesis, it will be important to analyze the structural features of the BGTC-containing lipoplexes at the various critical steps of their trafficking. In a broader perspective, the present study points out the need for and the importance of a "supramolecular galenics" approach to nonviral gene delivery, the development of which will probably require the simultaneous use of sophisticated biophysical techniques, cell-free models, subcellular fractionation techniques, etc. On the other hand, of crucial importance for the eventual clinical use of nonviral gene transfection approaches is the uncovering and exploitation of mechanisms of nuclear targeting and uptake. Both require progress in basic understanding of membrane and pore passage processes as well as empirical optimization of the insight gained.

We express our gratitude to C. Hélène and J. Navarro for their constant support and interest. We also thank P. Mailhé for technical help with the colloidal stability studies; P. Lesieur, D. Durand, and J. Doucet at LURE-DCI for help with the SAXS studies; J. P. Behr and M. Fauquet for critical reading of the manuscript; and J. C. Daniel, D. Escande, S. Fabrega, D. Roux, and E. Vivien for helpful discussions. This work was supported by grants from the Association Française de Lutte contre la Mucoviscidose, by the Association Française contre les Myopathies, and by the Bioavenir Program financed by Rhône-Poulenc, the French Ministry of Research, and the Ministry of Industry.

1. Lehn, P., Fabrega, S., Oudrhiri, N. & Navarro, J. (1998) *Adv. Drug Delivery Rev.* **30,** 5–11.
2. Miller A. D. (1998) *Angew. Chem. Int. Ed. Engl.* **37,** 1769–1785.
3. Vigneron, J. P., Oudrhiri, N., Fauquet, M., Vergely, L., Bradley, J. C., Basseville, M., Lehn, P. & Lehn, J. M. (1996) *Proc. Natl. Acad. Sci. USA* **93,** 9682–9686.
4. Oudrhiri, N., Vigneron, J. P., Peuchmaur, M., Leclerc, T., Lehn, J. M. & Lehn, P. (1997) *Proc. Natl. Acad. Sci. USA* **94,** 1651–1656.
5. Oudrhiri, N., Vigneron, J. P., Hauchecorne, M., Toury, R., Lemoine, A. I., Peuchmaur, M., Navarro, J., Lehn, J. M. & Lehn, P. (1998) *Biog. Amines* **14,** 537–552.
6. Soubrier, F. & Crouzet, J. (1997) *Eur. Pat. Appl.* WO 97 103, 43.
7. Pitard, B., Aguerre, O., Airiau, M., Lachagès, A. M., Boukhnikachvili, T., Byk, G., Dubertret, C., Herviou, C., Scherman, D., Mayaux, J. F. & Crouzet, J. (1997) *Proc. Natl. Acad. Sci. USA* **94,** 14412–14417.
8. Vinson, P., Talmon, Y. & Walter, A. (1989) *Biophys. J.* **56,** 669–681.
9. Templeton, N. S., Lasic, D. D., Frederik, P. M., Strey, H. H., Roberts, D. D. & Pavlakis, G. N. (1997) *Nat. Biotechnol.* **15,** 647–652.
10. Zabner, J., Fasbender, A. J., Moninger, T., Poellinger, K. A. & Welsh, M. J. (1995) *J. Biol. Chem.* **270,** 18997–19007.
11. Felgner, P. L. & Ringold, G. M. (1989) *Nature (London)* **337,** 387–388.
12. Gershon, H., Ghirlando, R., Guttman, S. B. & Minsky, A. (1993) *Biochemistry* **32,** 7143–7151.
13. Gustafsson, J., Arvidson, G., Karlsson, G. & Almgren, M. (1995) *Biochim. Biophys. Acta* **1235,** 305–312.
14. Labat-Moleur, F., Steffan, A.-M., Brisson, C., Perron, H., Feugeas, O., Furstenberger, P., Oberling, F., Brambilla, E. & Behr, J. P. (1996) *Gene Ther.* **3,** 1010–1017.
15. Lasic, D., Strey, H., Stuart, M., Podgornik, R. & Frederik, P. M. (1997) *J. Am. Chem. Soc.* **119,** 832–833.
16. Gao, X. A. & Huang, L. (1991) *Biochem. Biophys. Res. Commun.* **179,** 280–285.
17. Sternberg, B., Sorgi, F. L. & Huang, L. (1994) *FEBS Lett.* **356,** 361–366.
18. Rädler, J. O., Koltover, I., Salditt, T. & Safinya, C. R. (1997) *Science* **275,** 810–814.
19. Koltover, I., Salditt, T., Rädler, J. O. & Safinya, C. R. (1998) *Science* **281,** 78–81.
20. Litzinger, D. & Huang, L. (1992) *Biochim. Biophys. Acta* **1113,** 201–227.
21. Farhood, H., Serbina, N. & Huang, L. (1995) *Biochim. Biophys. Acta* **1235,** 289–295.
22. Wrobel, I. & Collins, D. (1995) *Biochim. Biophys. Acta* **1235,** 296–304.
23. Zhou, X. & Huang, L. (1994) *Biochim. Biophys. Acta* **1189,** 195–203.
24. Xu, Y. & Szoka, F. C. (1996) *Biochemistry* **35,** 5616–5623.
25. Demeneix, B. & Behr, J. P. (1996) in *Artificial Systems for Gene Delivery*, eds. Felgner, P. L., Heller, M. J., Lehn, P., Behr, J. P. & Szoka, F. C. (Am. Chem. Soc., Washington, DC), pp. 146–151.